Reaction Kinetics of Muonium with N_2O in the Gas Phase

James J. Pan,* Donald J. Arseneau, Masayoshi Senba,† Mee Shelly,‡ and Donald G. Fleming

TRIUMF and Department of Chemistry, University of British Columbia, 4004 Wesbrook Mall, Vancouver, BC, Canada V6T 2A3

Received: May 20, 1997; In Final Form: August 8, 1997[⊗]

The thermal reaction Mu + N_2O has been studied by the muon spin rotation (μSR) technique at temperatures from 303 to 593 K and pressures up to 60 atm. The overall reaction rate coefficient depends on the N_2O pressure quadratically in pure N_2O and is proportional to both the N_2O partial pressure and the total pressure in mixtures, confirming the theoretical prediction of Diau and Lin that the analogous H atom reaction proceeds through two channels in this temperature range, forming different products, MuN_2O and MuO + N_2. The measured total rate coefficients are much larger than those reported by Marshall et al. for H(D) + N_2O, indicating a dramatic kinetic isotope effect, which is mainly due to the enhanced quantum tunneling of the ultralight Mu atom. Even at room temperature (and low pressure), $k_{Mu}/k_H \approx 120$, the largest yet seen in comparisons of gas-phase Mu and H reactivity at such relatively high temperatures. The addition reaction forming MuN_2O (and by implication, HN_2O) contributes significantly to the total reaction rate at higher pressures but with the thermal rate coefficient remaining in the termolecular regime even at the highest pressures measured.

1. Introduction

The H + N_2O reaction has long been of interest in combustion chemistry.[1−8] Nitrous oxide is an important intermediate formed during propellant combustion[9] and is known to contribute to the depletion of stratospheric ozone.[10] The H + N_2O reaction, a key reaction in N_2O flames, is one of the few that can convert N_2O into N_2 thus avoiding production of undesirable nitrogen oxides in the atmosphere.[11] The development of chemical kinetic models to control N_2O formation is therefore highly desirable. To this end, it is essential to understand the temperature and pressure dependence of these reactions so that appropriate rate coefficients can be included in combustion models. Furthermore, the H + N_2O reaction has a very large activation barrier despite being highly exothermic, spin allowed, and symmetry allowed, and therefore is of fundamental interest.[4−7] The H(D) + N_2O reactions have been extensively studied experimentally,[1−3,12] but all of these, as well as earlier studies, were carried out at high temperatures (400−3000 K, some involved hot H/D atoms) and low pressures (mostly less than 1 atm). There are also several theoretical calculations of the rate coefficients for this reaction with different techniques.[1,3−6]

Despite the wealth of information available on this key reaction, the overall reaction mechanism and thus the dependence of the rate on pressure at different temperatures has yet to be established and confirmed by experiments.[1,5,6] At the relatively low pressures that have characterized the H(D) + N_2O experiments to date, no pressure dependence has been observed,[1] in contrast to recent theoretical predictions.[5,6] However, any expected pressure dependence would have been obscured by the small pressure ranges covered (55−430 Torr), especially in light of the tunneling effect which exhibits the opposite pressure dependence.[5] Furthermore, although significant isotope effects attributed to quantum tunneling were observed with H and D,[1] these atoms differ only by a factor of 2 in mass. A much greater tunneling effect can be expected for the analogous muonium reaction, Mu + N_2O, where the muonium atom, Mu, consisting of a positive muon (μ^+) and an electron, behaves chemically as an ultralight H isotope with only one-ninth the mass ($m_{Mu}/m_H = 1/9$).

The main distinction of Mu reaction kinetics compared with traditional hydrogen isotopes is the remarkable range and magnitude of kinetic isotope effects (KIEs) it is sensitive to. Because of its remarkably low mass, the quantum tunneling effect of the Mu atom, alluded to above, can be greatly enhanced relative to H(D), enabling observation of tunneling effects at easily accessible temperatures, indeed even at room temperature. Zero-point energy (ZPE) shifts, both at the transition states (TSs) and, in the present case, in the intermediate adduct, MuN_2O^*, also make significant contributions to the KIE. Another advantage in the study of Mu reactivity lies in the ease with which Mu atoms are formed by charge exchange in the gas,[13] which in turn facilitates measurements at high pressures. The wide and unprecedented pressure variation undertaken in the present study provides an invaluable probe of the total pressure dependence of H isotope + N_2O kinetics and enables us to distinguish contributions from different reaction channels. This is of considerable importance in comparison with current theoretical calculation of this reaction system.[5,6] Moreover, the muon spin rotation/relaxation (μSR) technique (see below) monitors Mu atoms individually, thereby eliminating the self-interactions that often plague H atom experiments.[12,14] The experimental Mu rate coefficients can thus be more accurate than those of their heavier atom counterparts (see, e.g., ref 15) and can, in principle, be used to predict H atom reaction rates, provided an accurate theory and potential energy surface are available.

The only previous measurement of the Mu + N_2O reaction was carried out in aqueous solution (H_2O saturated with N_2O) by Venkateswaran et al.[16] who reported a KIE on the order of 1000 in favor of the Mu atom at room temperature.

* To whom all correspondence should be addressed. E-mail: jjpan@triumf.ca. Fax: (604) 222-1074.

† Present address: Department of Physics, Dalhousie University, Halifax, NS, Canada.

‡ Present address: Department of Chemistry, Miami University, Oxford, OH 45056.

⊗ Abstract published in *Advance ACS Abstracts,* October 15, 1997.

S1089-5639(97)01677-0 CCC: $14.00

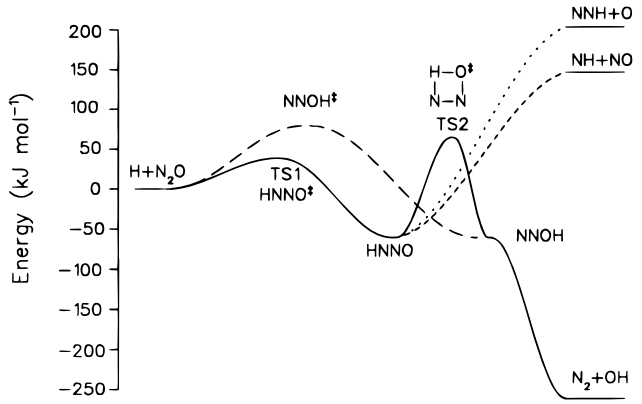

Figure 1. Reaction coordinates and energetics for H + N_2O, adopted from refs 1 and 5 (cf. text). The zero-point energies are included.[5]

2. The Reaction Mechanisms and the μSR Technique

A. Reaction Pathways of H(Mu,D) + N_2O. The H + N_2O reaction[17] has four possible products as shown in the potential energy diagram of Figure 1, adapted from the energetics given in refs 1 and 5, which suggests that the major reaction channels, particularly at lower temperatures, would be those forming N_2 + OH or HNNO.The reaction forming HNNO involves addition of H to the N end of N_2O and passing through the HNNO‡ transition state (TS1) to form the excited HNNO* intermediate which is then stabilized by collisions,

$$\mathrm{H + N_2O \rightleftharpoons HNNO^* \xrightarrow{M} HNNO} \qquad (1)$$

Both HNNO* and HNNO may undergo a 1,3-hydrogen shift to form (via TS2, assisted by tunneling) the unstable NNOH intermediate, which dissociates to N_2 + OH, but the rate depends strongly on internal excitation, with stabilized HNNO reacting much more slowly. Depending on the time scale of the experiment, HNNO may be regarded either as a relatively stable reaction intermediate or as a "final" product. Consistent with the calculations in ref 5, the results presented in this article are interpreted by regarding HNNO (and MuNNO) as a final product and hence with addition and stabilization considered as a distinct reaction channel. The addition channel has an enthalpy barrier of 38 kJ/mol at 300 K and is exothermic, $\Delta H_0 = -61$ kJ/mol, for forming stable HNNO (though much less so for MuNNO). It is unusual in that the formation of HNNO has a higher effective Arrhenius *A* factor than the reverse unimolecular dissociation, a result of the low entropy of the reactant H atom combined with loss of a rotor in the dissociation.[1,6] Thus, with a relatively small dissociation coefficient, HNNO* can be expected to have a high probability of either stabilization or tunneling through the second barrier (TS2). The recent theoretical calculations have shown that the addition channel is important at even 200 Torr total pressures,[5,6] in contrast to earlier experiments which concluded that it is not a major pathway based on a reported pressure independence of the reaction rate coefficient.[1] The present results for the Mu + N_2O reaction, however, clearly establish the importance of pressure-dependent pathways in the overall mechanism.

The reaction forming N_2 + OH, with $\Delta H_0 = -261$ kJ/mol, is highly exothermic overall,[5] but also exhibits high reaction barriers. There are two pathways for this reaction to proceed, a "direct" pathway and an "indirect" one, shown by the long-dashed and solid lines, respectively, in Figure 1. The direct pathway is the addition of an H atom to the O end of N_2O (with the transition state NNOH‡) to form the unstable NNOH intermediate which immediately dissociates to N_2 and OH. The calculated enthalpy barrier relative to the reactants for this direct process is 76 kJ/mol at 300 K.[5] Note that this direct mechanism is distinct from simple abstraction, where the initial H attack at the O atom with simultaneous weakening of the N−O bond would lead to a large preexponential factor in the Arrhenius expression due to the loose transition state.[1] This channel should have no pressure dependence since NNOH is not a stable product. At temperatures above 1000 K, calculations show that this channel contributes significantly to the overall reaction rate coefficient but it is not expected to account for the observed rate coefficient at lower temperatures.[1,6]

The alternate indirect mechanism shares the first step with the addition channel that forms the HNNO* intermediate. This step is followed by a 1,3-hydrogen shift to form the unstable NNOH intermediate (via TS2), which dissociates with an enthalpy barrier of 64 kJ/mol relative to H + N_2O. At lower temperatures, the indirect pathway is favored over the direct one since it is much easier to tunnel through the lower first barrier (TS1) and particularly the narrower second barrier (TS2) of the indirect process.[1,4,6,8,18] The H data, despite the absence of any moderator pressure dependence, agree much better with the indirect model than the direct model calculations below 1000 K.[1,6] The tunneling effect is dramatic because the intermediate (HNNO*) precursor to the 1,3-hydrogen shift transition state gives rise to a large (but narrow) internal barrier of 126 kJ/mol relative to the HNNO ground state. The formation rate of N_2 + OH through this indirect channel is dependent on the total pressure because the collisional activation/deactivation of HNNO* affects both the classical overbarrier and quantum tunneling reaction rates for forming NNOH.

The reactions forming NH + NO and NNH + O are both highly *endo*thermic with reaction enthalpies of about 147 and 203 kJ/mol at 300 K, respectively,[5] and thus are not important contributions to the thermal reaction rates near room temperature.

The isotopic reaction Mu + N_2O is expected to proceed in the same fashion as that for H + N_2O, represented by the following scheme:

$$\mathrm{Mu + N_2O \xrightarrow[MuONN^{\ddagger}]{k'_d} MuO + N_2} \qquad (2)$$

$$\mathrm{Mu + N_2O \xrightarrow[MuNNO^{\ddagger}]{k_a} MuNNO^*} \qquad (3)$$

$$\mathrm{MuNNO^* \xrightarrow[MuNNO^{\ddagger}]{k_{-a}} Mu + N_2O} \qquad (4)$$

$$\mathrm{MuNNO^* + M \xrightarrow{\beta k_s[M]} MuN_2O + M} \qquad (5)$$

$$\mathrm{MuNNO^* \xrightarrow[\substack{Mu\text{-}O^{\ddagger}\\ |\quad |\\ N\text{-}N}]{k_d} MuO + N_2} \qquad (6)$$

where the *k*s are rate coefficients for each particular process and β is the efficiency of collisional stabilization in the "strong collision" model.[19] From either an eigenvalue solution or the steady-state approximation, the total thermal rate coefficient for the overall chemical reaction of Mu is found[20] to have the form:

$$k_c = k'_d + \frac{k_a(k_d + \beta k_s[M])}{k_{-a} + k_d + \beta k_s[M]} \qquad (7)$$

where k_c is defined by $-\mathrm{d[Mu]}/\mathrm{d}t = k_c[N_2O][Mu]$. This expression exhibits the usual expected chemical kinetics limits.

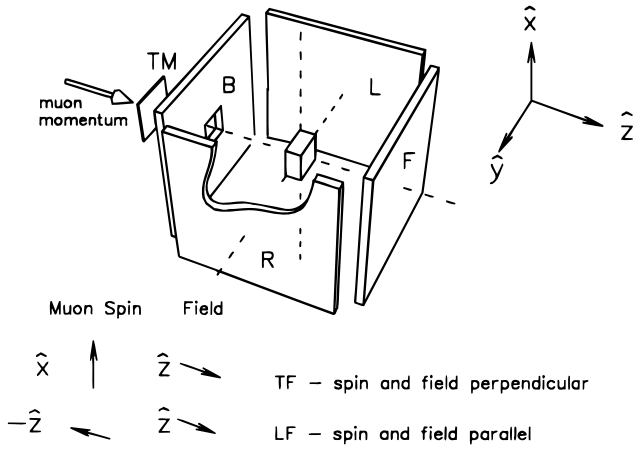

Figure 2. Schematic of a μSR experiment. TM is the muon counter. B, L, F, and R are positron counters. The arrows under the column labeled "muon spin" indicate the muon spin direction while the arrows under the column "field" show the direction of the applied magnetic field. The gas target positioned in the center of the counters is actually much larger than indicated in the figure.

Thus, when k_{-a} is much larger than $\beta k_s[M] + k_d$ (the low-pressure limit, indicated over the range of pressures run), and k'_d, the contribution from the direct pathway, is small (this is as expected from the earlier discussion for H, and ZPE conceivably could raise the barrier height further for Mu), eq 7 reduces to

$$k_c = k_1 + k_2[M] \tag{8}$$

with

$$k_1 = \frac{k_a k_d}{k_{-a}} \tag{9}$$

$$k_2 = \frac{k_a \beta k_s}{k_{-a}} \tag{10}$$

where k_1 is the overall bimolecular rate coefficient for MuO + N_2 formation and k_2 the termolecular rate coefficient for MuN_2O stabilization. Note that the moderator "M" here can be either N_2O itself or some added inert gas (N_2 or Ar in this study).

B. μSR Technique. The gas chemistry time-differential μSR techniques[20−22] utilize 100% spin-polarized muons produced in the parity-violating pion decay processes. When these spin-polarized muons (with a few MeV initial energy) enter a reaction cell filled with gases, they slow down and thermalize. Some muons emerge as thermalized Mu atoms, also spin-polarized.[13,20,24] In a μSR experiment, the reaction rate is measured by monitoring the disappearance of spin-polarized Mu atoms via the detection of muon decay positrons ($\mu^+ \rightarrow e^+\nu_e\bar{\nu}_\mu$), which are emitted along the muon spin direction in either a transverse (TF) or longitudinal (LF) magnetic field (see Figure 2). A clock is started by an incoming muon and stopped by the detection of a positron in any of the counters. The electronic logic of the data acquisition system ensures that there is only one muon in the target at a time so the muon that created each decay positron is unambiguously identified. The time histogram of detected positrons, $N(t)$, from a single counter can be fit to the following form

$$N(t) = N_0 e^{-t/\tau_\mu}[1 \pm A(t)] + N_B \tag{11}$$

where N_0 is a normalization factor, τ_μ is the muon lifetime (2.197 μs), N_B is a constant to account for time-independent background, and $A(t)$ is the muon decay asymmetry which accounts

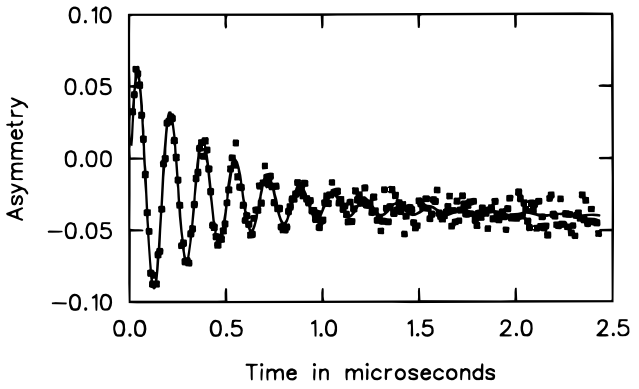

Figure 3. A typical TF experimental μSR signal after removal of normalization, decay, and background. The spectrum was obtained in 22 atm pure N_2O at 303 K and 5 G TF. The solid line is a fit to eq 12. It is primarily the relaxation rate "λ" which is of interest.

for the time dependence of the muon polarization and contains the kinetics information of the reaction. In general, $A(t)$ has the form

$$A(t) = \sum_i A_i e^{-\lambda_i t} \cos(\omega_i t + \phi_i) \tag{12}$$

where the index i labels each magnetic environment of the muon: paramagnetic Mu (i = Mu), a diamagnetic molecule (i = D), or a paramagnetic Mu-containing radical (i = R). The parameters A_i, λ_i, ω_i, and ϕ_i are, respectively, the initial asymmetry, the relaxation rate, the Larmor precession frequency (equals zero in a LF), and the initial phase of the spin polarization of muons in the i-th environment.[20−24] A typical μSR signal obtained in a weak TF is shown in Figure 3, giving the relaxation rate, λ, of principal interest in the present experiments.

μSR is essentially a spin-depolarizing technique: *any* mechanism which perturbs the coherent precession of triplet Mu spin in a weak TF or causes "spin flip" in a LF gives rise to relaxation of the signal.[20] Most of the work in the present study was carried out in a weak TF environment, where polarization loss is essentially one of spin dephasing, described by eq 12. Since N_2O has no unpaired electron, there is no intermolecular spin exchange interaction causing relaxation as there is, for example, in the case of Mu + NO.[22] However, in a transverse magnetic field, when Mu enters one of the two long-lived product species MuO and MuN_2O, both free radicals, it rapidly loses phase coherence with the reactant Mu ensemble (T_2) because either the hyperfine interaction with nuclear moments splits the precession frequency, similar to the case of MuC_2H_4,[27−29] and/or concurrently it undergoes rapid collisional spin relaxation (T_1), primarily due to the electronic spin-rotation interaction.[20,28] The OH radical is difficult to observe even in liquid-phase electron spin resonance (ESR) due to its large spin rotation interaction.[30] Current studies in our research group,[20,28,31−34] as well as theoretical studies of spin relaxation of muonium free radicals,[29] have demonstrated extremely fast relaxation rates (extrapolated) in weak magnetic fields, particularly for small radical systems. The spin relaxation of free radicals can only be followed in a LF of appreciable strength ($\gtrsim$1 kG).[20,28,31] Nonetheless, the spin−rotation coupling in the MuNNO radical is not as strong as in some smaller radicals, e.g., MuO and MuCO. Unlike the reaction of Mu + CO,[32] the Mu relaxation rate due to spin−rotation coupling in the short-lived intermediate MuNNO* is much smaller than the chemical reaction rate (k_c) and can be neglected. The above assessment is confirmed by the fact that the measured relaxation rates have no field

dependence in up to 100 G TF (see below). Thus, the Mu spin relaxation rate observed in a weak TF (<10 G) is just the total disappearance rate of Mu due to chemical reactions, $\lambda_{Mu} \equiv -\mathrm{d[Mu]/[Mu]d}t$), and is given by (see eq 8):[20]

$$\lambda_{Mu} = \lambda_0 + k_c[N_2O] = \lambda_0 + (k_1 + k_2[M])[N_2O] \quad (13)$$

where λ_0 is a very slow background relaxation caused by such factors as magnetic field inhomogeneity.

Though N_2O itself is diamagnetic and so cannot undergo (intermolecular) spin exchange, paramagnetic impurities in the gas could do so, and since both the spin exchange (or intramolecular spin relaxation) and the chemical reaction can give rise to relaxation of the μSR signal, it is important that these different processes are clearly identified in order to properly extract the kinetics.[20,32] The traditional method for doing this is in a LF environment, where the "decoupling" of the muon and electron spins effects a separation as exemplified in our recent study of Mu + NO.[22] It has also recently been established that a similar separation can be effected in TF environment by comparing the μSR relaxation rates in weak (<10 G) and intermediate (30−100 G) magnetic fields. The relaxation rates due to spin exchange (or intramolecular spin relaxation, e.g., spin−rotation coupling in the short-lived intermediate) differ by a factor of 1.5 because the fraction of coherently precessing Mu atoms is different, while the relaxation rates due to chemical reactions, on the other hand, stay constant with field strength variation.[20,32,35,36]

3. Experimental Section

The experiments were performed with "surface muons" on the M15 beamline of the TRIUMF cyclotron[32] in weak (6 or 8 G) and intermediate (40 or 100 G) transverse magnetic fields. The experimental setup was similar to other gas μSR experiments, as described in detail in refs 20−24, 35, and 38 and schematically shown in Figure 2. Mu relaxation rates were measured in pure N_2O at pressures from 1.2 to 51 atm and in mixtures of N_2O and N_2 (and/or Ar) with total pressures up to 60 atm. In addition to the room temperature (303 K) studies, reaction rates were also measured at 403, 496, and 593 K at pressures below 17 atm. Some measurements were also done in LF from 0.01 to 19.2 kG at room temperature.

Two separate reaction vessels were used. Briefly, room temperature experiments were conducted using a high-pressure (≤60 atm) chamber which was an aluminum cell approximately 15.6 cm (10 cm inside) long with a 9.5 cm inside diameter.[21,22] The muon beam entered the target cell through a 1.1 cm diameter, 100 μm thick window bored out of the 2.7 cm thick titanium end flange. The high-carbon 316 stainless steel vessel described in ref 38 was used in the high-temperature measurements, with the same heating and temperature control systems as described therein. This cell was used for temperatures up to 600 K and pressures to 17 atm.

Though kinetically much faster than its H + N_2O counterpart, the reaction rate of N_2O with muonium is still very slow, so even a small contamination of the gases used could cause significant errors in the result. The N_2O gas (Canadian Liquid Air, research grade purity, ≥99.995%) was freeze−pump−thawed (more than three times) at the beginning of each run period until the impurities fell below a level at which no significant contributions from impurities to the relaxation rate could be observed. This was done both by repeating runs with the same N_2O pressure before and after a cycle of freeze−pump−thaw and by confirming the absence of spin exchange reactions utilizing the field variation method outlined above and described in more detail in refs 20, 35, and 36 (likely impurities, NO, O_2, and NO_2, are all paramagnetic and will relax the Mu signal by spin exchange, but N_2O itself only undergoes chemical reactions with Mu[36]). Similarly, the experimental data showed that the thermal decomposition of N_2O ($N_2O + M \rightarrow N_2 + O + M$) is very slow over the temperature range concerned[39] and had no significance. It is emphasized that the experimental results were indeed very well reproduced with completely different setups (different target vessels, gas bottles, and spectrometers, see Figure 4).

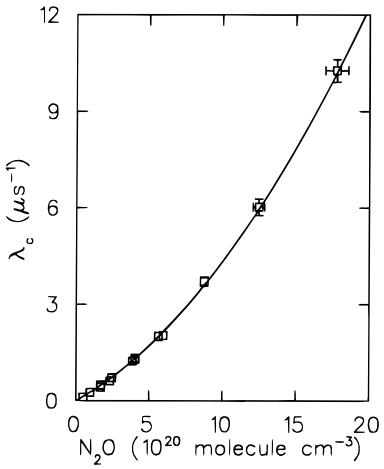

Figure 4. TF relaxation rates for the Mu + N_2O reaction at 303 K for different pure [N_2O]. The solid line is a fit of the data to eq 14. Most of the data were measured using the high-pressure target vessel while the high-temperature target vessel was used for some low-pressure points as described in the text. The reproducibility is very good (note the overlapping points).

The source of uncertainty in the N_2O concentration ([N_2O]) is mainly the uncertainty in measuring its pressure and the temperature in the target. Target temperatures were monitored and controlled by a temperature controller with thermocouple readings of the temperatures at various locations on the reaction cell. Temperature uncertainty was well below 3 K, but considering the slow drifting with time over the course of a given run, 3 K is used as the upper limit of absolute uncertainty in temperature. The pressures under 13 atm were measured with two different MKS baratron capacitance manometers, depending on the range, with uncertainties less than 0.6%. Higher pressures, up to 60 atm, were measured with a "Marsh" gauge to an absolute accuracy of <0.1 atm. An upper limit of 1% error in pressure is used in the analysis. Another possible source of error lies in the conversion of pressure to concentration. N_2O deviates from an ideal gas at pressures higher than about 10 atm at room temperature (less so at higher temperatures), so the van der Waals equation, using parameters taken from ref 40, was used to calculate concentrations from measured pressures. The compressibility curves yield essentially the same values. A generous allowance for the combined error in [N_2O] from all sources is taken as ±5%, which is used in the data analysis.

4. Results and Discussion

A. Mu Results. The reaction rates measured at 303, 403, 496, and 593 K in pure N_2O with pressures from 1.2 to 51.4 atm are listed in Table 1 and plotted in Figures 4 and 5. Since these data were taken at different times over a span of about two years with different target vessels and μSR spectrometers, giving various background relaxation rates (λ_0), the values given here are background-corrected ($\lambda_c = \lambda_{Mu} - \lambda_0$) and are weighted averages for the two counters used. The values of λ_0 for each

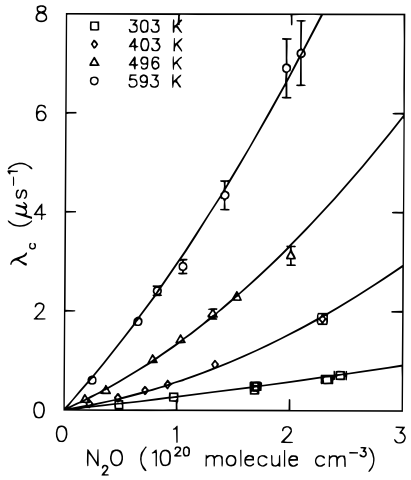

Figure 5. TF relaxation rates for Mu + N_2O at different temperatures and vs concentration of pure N_2O. The solid lines are fits of the data to eq 14. These data were measured with the high-temperature target vessel except a few points at 303 K. High-pressure data at 303 K are not included in the plot (see Figure 4) but the fit included all data points.

TABLE 1: Transverse Field Relaxation Rate of Mu + N_2O

[N_2O] (10^{20} molecule cm^{-3})	total pressure (atm)	temp (K)	λ_c (μs^{-1})
0.4888 ± 0.0099	2.00	303	0.1186 ± 0.0087
0.976 ± 0.020	4.00	303	0.277 ± 0.013
1.688 ± 0.035	6.83	303	0.487 ± 0.031
1.691 ± 0.035	6.84	303	0.427 ± 0.032
1.691 ± 0.035	6.84	303	0.495 ± 0.024
1.695 ± 0.035	6.85	303	0.503 ± 0.021
1.712 ± 0.036	6.86	303	0.498 ± 0.017
2.333 ± 0.050	9.33	303	0.635 ± 0.033
2.449 ± 0.053	9.50	303	0.725 ± 0.022
3.872 ± 0.088	14.6	303	1.239 ± 0.041
4.039 ± 0.092	15.3	303	1.289 ± 0.063[a]
4.039 ± 0.092	15.3	303	1.332 ± 0.059
5.65 ± 0.14	21.0	303	2.012 ± 0.061
5.96 ± 0.15	21.6	303	2.048 ± 0.058
8.75 ± 0.24	30.6	303	3.72 ± 0.14
12.46 ± 0.40	40.4	303	6.03 ± 0.26
17.76 ± 0.77	51.4	303	10.27 ± 0.35
0.2265 ± 0.0039	1.24	403	0.096 ± 0.016
0.4799 ± 0.0085	2.62	403	0.219 ± 0.016
0.720 ± 0.013	3.92	403	0.367 ± 0.028
0.921 ± 0.016	5.00	403	0.485 ± 0.024
1.339 ± 0.024	7.24	403	0.899 ± 0.036
2.289 ± 0.042	12.2	403	1.827 ± 0.11
0.1857 ± 0.0030	1.25	496	0.218 ± 0.016
0.3719 ± 0.0060	2.50	496	0.395 ± 0.016
0.785 ± 0.013	5.26	496	1.023 ± 0.039
1.033 ± 0.017	6.93	496	1.431 ± 0.042
1.317 ± 0.022	8.79	496	1.956 ± 0.099
1.530 ± 0.025	10.2	496	2.296 ± 0.076
2.006 ± 0.033	13.3	496	3.13 ± 0.19
0.2499 ± 0.0038	2.02	593	0.660 ± 0.026
0.6539 ± 0.0099	5.26	593	1.852 ± 0.069
0.824 ± 0.013	6.63	593	2.68 ± 0.13
1.049 ± 0.016	8.43	593	2.96 ± 0.14
1.418 ± 0.022	11.4	593	4.40 ± 0.29
1.958 ± 0.030	15.6	593	6.97 ± 0.59
2.087 ± 0.032	16.7	593	7.27 ± 0.65

[a] Intermediate magnetic fields (40−100 G).

particular set of data were obtained by fitting the data to eq 13, which were found to be the same as the measured λ_0 values in pure moderators, within the uncertainties of these measurements. The corrected relaxation rates at each temperature were fit to the following functional form, expected from the overall reaction mechanism discussed above (see eq 13):

$$\lambda_c = k_1[N_2O] + k_2[N_2O]^2 \quad (14)$$

Results of these fits are listed in Table 2. It should be recalled that the parameters k_1 and k_2 are the rate coefficient ratios given by eqs 9 and 10, respectively. A typical plot is shown in Figure 4 for data taken at 303 K and up to 52 atm pure N_2O pressure. The temperature dependence is shown in Figure 5 for pressures up to 17 atm.

According to the calculations of Diau and Lin,[5] k_{dec} (k_1) is not a true "constant" but one that decreases with total pressure due to collisional deactivation. It is also predicted in the same reference that for H(D) systems with Ar as moderator at pressures above a few hundred Torr the addition reaction is in the falloff region and the rate coefficient k_{add} (k_2[M]) does not increase with pressure linearly as implied by eqs 8 and 10. However, the present Mu data do not show any deviation from a linear dependence on moderator pressures in pure N_2O (Figure 5).[41] The moderator effects were also measured using N_2 and Ar gases. The results are listed in Table 3 and selectively plotted in Figure 6. At very low total pressures *no* significant moderator pressure dependence was observed, consistent with the H + N_2O data in ref 1. At higher total pressures and room temperature, the observed relaxation rates increased with total pressure linearly (Figure 6) in N_2, except one point at the highest pressure (not shown). The linear dependence can only come about if k_{dec} does not decrease with total pressure (so in fact k_1 *is* a true constant) *and* k_{add} increases linearly with moderator pressure; in other words, the addition reaction is still in the low-pressure (termolecular) regime. On the other hand, in a high-pressure Ar moderator (and one point in N_2), k_c did actually decrease with increasing moderator pressure (consistent with the results for k_{dec} in ref 5). It could be that collisional deactivation sufficiently alters the energy distribution in the HNNO well at the highest pressures, that the contribution to MuO formation from quantum tunneling is decreased faster than the increasing contribution to MuN_2O formation. The effect seems most dramatic with an Ar moderator, but both future studies and detailed theoretical calculations are required to confirm the trend, so those results will not be discussed further in this paper.

As noted, some data were taken in longitudinal fields at room temperature, the analyses of which is reported elsewhere.[31] The LF relaxation rates typically contain more than one relaxing component at some fields, which is consistent with the aforementioned reaction mechanisms. The details are not important here but it should be noted that the data showed that both a chemical process (λ_c) and a free radical collisional spin interaction (λ_R) contribute to the LF relaxation rates, with the latter being strongly field-dependent. This is consistent with a detailed analysis of the spin relaxation of the Mu−ethyl radical.[28] In principle, from an analysis of the fitted amplitudes and relaxation rates in a LF, corroborating evidence supporting the interpretation below can be obtained,[20] but additional data is required to confirm this. The important point here is that the large relaxation rates seen in weak TF are the consequences of and evidence for spin rotational relaxation in the product radicals, meaning that in a TF, where there is only *one* relaxing component, any stable MuO or MuN_2O formed will effect an essentially instantaneous relaxation on the time scale of Mu precession. This is the basis of eq 13. The results and discussion to follow are based entirely on the TF data.

To compare with the H(D) data, which were obtained at much lower pressures (less than 430 Torr), total Mu reaction rate coefficients are extrapolated to 200 Torr total pressure, using eq 8 and the parameters listed in Table 2, with [M] being fixed

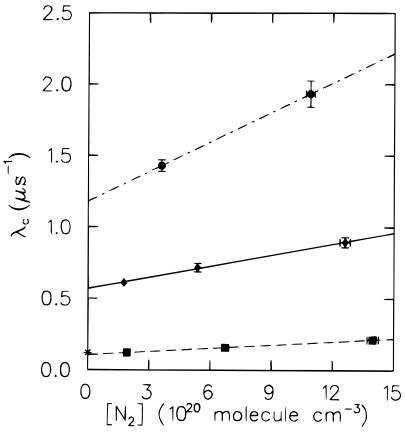

Figure 6. N_2 moderator pressure dependence for the Mu + N_2O reaction at 303 K. N_2O concentrations are 0.49 (squares, dash line), 1.93 (diamonds, solid line), and 3.71 (circles, dash−dot line) × 10^{20} molecule cm^{-3}. The asterisk is the pure N_2O (0.49) data point. This positive linear dependence was observed at all but the highest N_2O concentration for N_2 moderator. Both the intercepts and slopes in Figure 6 are also linearly dependent on N_2O concentration as expected ([N_2O] is too small to see the quadratic [N_2O] dependence of the intercept, see Figure 4).

TABLE 2: Rate Coefficients of the Mu + N_2O Reaction

T (K)	k_1 (10^{-14} cm^3 molec^{-1} s^{-1})	k_2 (10^{-34} cm^6 molec^{-2} s^{-1})
303	0.252 ± 0.005	0.018 ± 0.001
403	0.361 ± 0.028	0.205 ± 0.039
496	1.014 ± 0.053	0.325 ± 0.066
593	2.540 ± 0.080	0.433 ± 0.100

TABLE 3: Moderator Dependence of Relaxation Rates.

[N_2O] (10^{20} molecule cm^{-3})	total pressure (atm)	temp (K)	λ_c (μs^{-1})
	M = N_2		
0.4888 ± 0.0099	10.0	303	0.1192 ± 0.0082
0.4888 ± 0.0099	30.0	303	0.156 ± 0.013
0.4888 ± 0.0099	60.0	303	0.211 ± 0.016
1.929 ± 0.041	15.0	303	0.649 ± 0.022
1.929 ± 0.041	30.0	303	0.717 ± 0.030
1.929 ± 0.041	60.0	303	0.896 ± 0.035
3.705 ± 0.067	29.25	303	1.430 ± 0.040
3.705 ± 0.067	59.52	303	1.933 ± 0.093
8.75 ± 0.24	40.41	303	4.96 ± 0.30
8.75 ± 0.24	59.86	303	4.30 ± 0.17
0.2187 ± 0.0038	12.24	403	0.0953 ± 0.0073
0.2499 ± 0.0038	12.9	593	1.116 ± 0.034
	M = Ar		
1.929 ± 0.041	30.0	303	0.582 ± 0.021
1.929 ± 0.041	60.0	303	0.466 ± 0.024
0.6539 ± 0.0099	9.57	593	2.204 ± 0.093
0.824 ± 0.013	9.26	593	3.67 ± 0.18
0.824 ± 0.013	12.0	593	3.44 ± 0.17
0.824 ± 0.013	15.0	593	3.15 ± 0.20
	M = Ar/N_2		
0.2499 ± 0.0038	10.0/13.0	593	0.915 ± 0.033
0.6539 ± 0.0099	9.57/15.0	593	2.432 ± 0.099

at a corresponding value. These are plotted along with the H(D) experimental results[1] in Figure 7. A similar comparison but with the H(D) theoretical calculations of ref 5 at higher pressures is shown in Figure 8. This procedure facilitates direct comparison between the H(D) + N_2O data and Mu + N_2O experiment at the same total pressure, since the experimental data were obtained over a range of pressures (Tables 1 and 3), giving the fitted parameters in Table 2.

B. Comparison with H(D) + N_2O. Among the many experimental studies of the kinetics of the H(D) + N_2O reaction, the results of Marshall et al.[1] are the most recent thermal rate

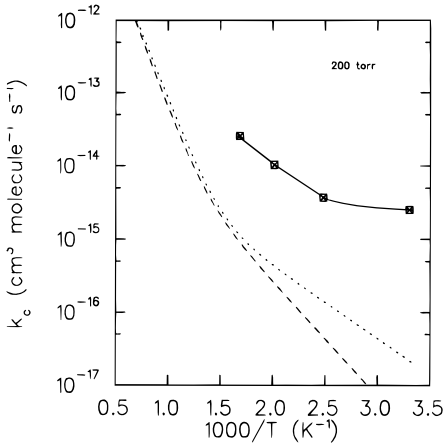

Figure 7. Arrhenius plot of total rate coefficient for the Mu + N_2O reaction at 200 Torr. The dot and dash lines are, respectively, H and D experimental data.[1] The points indicating the Mu data are not actual data points at this pressure but are obtained from the fitted parameters at higher pressures, and the solid line is simply drawn here to guide the eye.

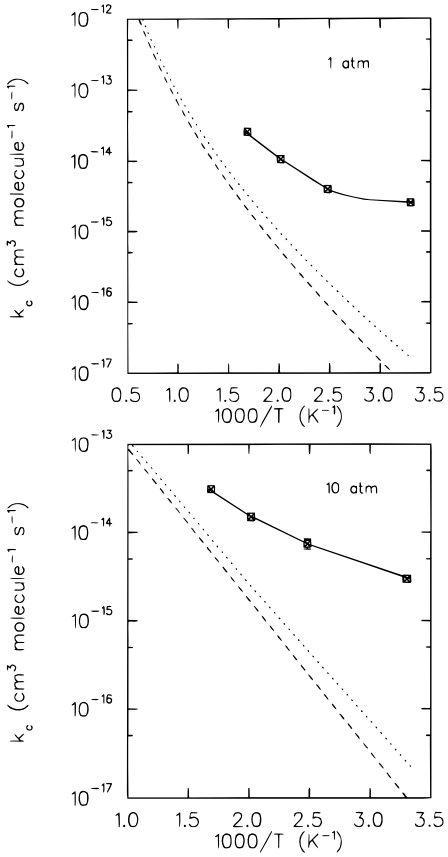

Figure 8. Same as Figure 7 but at higher pressures. In this case though the dot and dash lines are theoretical calculations for H and D + N_2O.[5]

coefficient measurements and the most relevant here. Their study is one of the few that have covered lower temperature ranges (390−1310 K) and is the only isotope effect study under thermal conditions similar to the present μSR experiments. They employed a high-temperature photochemistry technique in which time-resolved resonance fluorescence spectroscopy was used to monitor the reduction in concentration of H(D) generated by flash photolysis of $NH_3(ND_3)$ in a reactor containing mixtures of N_2O and Ar. The total pressure was between 55 and 430 Torr (Ar as moderator). They found empirical fits to a sum of two activation energies and concluded that the overall reaction rate coefficients were *pressure-independent*. The results from

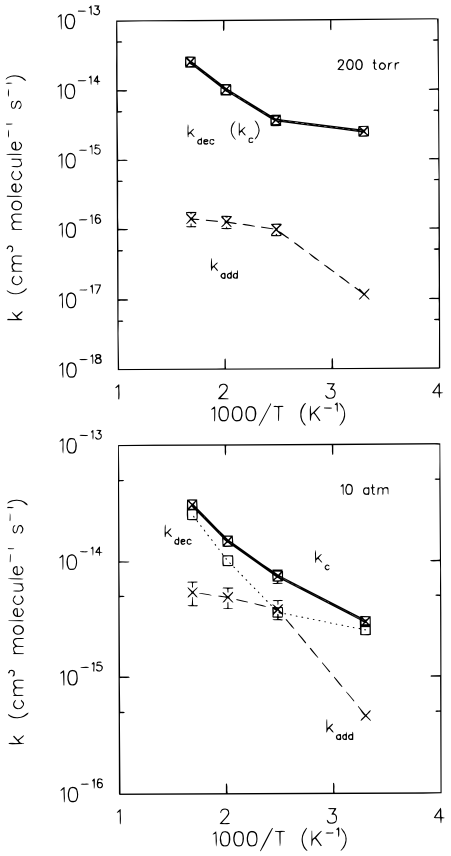

Figure 9. Comparison of contributions from the addition (crosses, dashed line) and decomposition (squares, dotted line) channels to the total rate coefficient (cross-in-squares, double-solid line) for the Mu + N_2O reaction. Total (pure N_2O) pressures are as indicated.

their fits are plotted in Figure 7 along with the results of fits to the present Mu data at 200 Torr. Marshall et al. also presented some theoretical considerations and a BAC-MP4 calculation[10,42] using a model involving rearrangement of an HNNO intermediate coupled with tunneling through an Eckart potential barrier. The distinct curvature of the Arrhenius plot seen at lower temperatures in Figure 7 for H(D) + N_2O was attributed to the effect of quantum tunneling due to the H(D) atom 1,3-migration process, following initial thermal addition to the N atom. This is the "indirect mechanism" referred to earlier. Even at their higher temperatures, they dismissed both endothermic reaction channels, forming NNH + O and NH + NO, and argued, based on the lack of pressure dependence, that the addition channel was not a major pathway either. They also neglected any tunneling through the first barrier in the indirect pathway.

However, two recent theoretical calculations for H(D) + N_2O have indicated that the addition channel *is* important, even dominant, at lower temperatures over the pressure range of the experiment of Marshall et al.[5,6] Diau and Lin[5] also argued that the curvature in the Arrhenius plot of the H(D) experimental data (Figure 7) is mainly due to a change of dominant mechanism, from decomposition to addition at low temperatures.

The present Mu data is invaluable here in establishing the reaction mechanism because contributions from the addition and decomposition channels can be unambiguously distinguished by the large pressure range investigated. The quadratic dependence on [N_2O], indicated by eq 14 for pure N_2O (seen in Figure 4), are extracted from the global fits to the data, yielding the separate rate coefficients $k_1 = k_{dec}$ and $k_2 = k_{add}$/[M] from the fitted parameters given in Table 2. These are plotted in Figure 9 for different N_2O pressures. In contrast to the calculations for H + N_2O,[5] which predict that addition should be dominant at low temperatures, even at low pressures, for Mu at low pressures, the dominant channel is *decomposition*, $k_{dec} = k_1$, at *all* temperatures; k_{add} is important only at pressures higher than a few atmospheres. Moreover, the curvature in the Arrhenius plot of total rate coefficient, most apparent at 200 Torr, is *not* merely due to a change in dominant channel between addition and decomposition as suggested by Diau and Lin[5] for H(D) but due to a quantum tunneling effect in the decomposition reaction. This conclusion tends to support the similar conclusion of Marshall et al. for H(D) + N_2O,[1] even allowing for the marked enhancement in quantum tunneling that Mu undergoes.

What can be directly compared then with the H(D) experimental data, all obtained at *low* pressures, are the decomposition rate coefficients, since the addition rate coefficients are negligibly small in those studies (Figure 9). At all temperatures, but particularly at low temperatures, the Mu + N_2O decomposition rate coefficient k_{dec} is much larger than those of the H(D) systems, as can be seen in the comparative plots given in Figure 7. At 300 K, the ratio of extrapolated rate coefficients (k^M_{dec}/k^H_{dec}) is 120, the largest KIE yet reported in comparative studies of Mu and H in the gas phase near room temperature[23] (this ratio would in fact be an order of magnitude higher if the theoretical calculations of Diau et al.[5] were used). Even at 500 K, the ratio is still 23, whereas at this temperature, k^H_{dec}/k^D_{dec} is only 1.7, though still larger than the classical ratio of 1.4. It is worth emphasizing, as discussed by Marshall et al.,[1] that there *is* indeed appreciable tunneling for the H(D) + N_2O reaction, perhaps more than is commonly seen at such relatively high temperatures.

The isotope effect (k^{Mu}/k^H) reported in previous μSR studies in liquid water,[16] on the order of 1000 at 300 K, is an order of magnitude higher than seen here in the gas phase. While it seems surprising, an enhancement of this order in the comparisons of reaction rate coefficients in solution and in gases is not inconsistent with previous comparison of Mu (and H) atom reactivity in these different media.[43] However, the mechanism is not at all clear in the study reported in ref 16. In solution, the Mu + N_2O reaction can be expected to be dominated by MuN_2O formation, based on the results presented above. Moreover, as found in our present study, impurities in the N_2O gas, particularly O_2 (and NO), if not properly degassed, could introduce significant and erroneous relaxation rates due to their large spin-exchange cross sections.[35,22] The fact that the N_2O in the liquid-phase μSR study was used from source without any further purification (a bubbling technique was used to degas the solvent in ref 16) and that the measurement is based on only one (indirectly determined) N_2O concentration[16] casts doubt on the size of the reported KIE. It would be of interest, in view of the apparently dramatic effect on reactivity, to repeat the experiment over a range of concentrations (and temperatures).

In general, kinetic isotope effects can originate from two broad possible sources: zero-point energy (ZPE) shifts, either in the reactant molecule or at the transition state, and tunneling. In most cases of Mu reactivity the ZPE shift at the transition state is important, especially for endothermic reactions with late ("tight") transition states, often leading to an "inverse" KIE, with $k_{Mu} \ll k_H$, exemplified by Mu + H_2[44] and Mu + CH_4.[38] However, in the present case, since the intermediate molecule following TS1 in the indirect pathway is the reactant for the second barrier (Figure 1), the increased ZPE for Mu, combined with a reduced density-of-states, may give a "normal" KIE, favoring the lighter Mu atom. In terms of the (classical) activation energy, E_a, this also means that the effective E_a may be pressure-dependent for both H(D) and Mu + N_2O but particularly Mu + N_2O, possibly giving rise to a larger E_a, hence

reduced rate coefficient, at high pressures. Contributions due to quantum tunneling, the second important mass effect which always favors lighter atoms and is itself pressure-independent, are also reduced at higher pressures due to different energy distributions in the intermediate MuNNO*. Both these effects may partly explain the anamolous moderator dependence noted earlier in the case of Ar.

The huge KIE reported here for k_{Mu}/k_H can be explained by pronounced quantum tunneling of Mu, in principle through both barriers of the "indirect" pathway leading to MuO formation (Figure 1). However, while Mu tunneling through the wider first barrier (TS1) could be important, tunneling through the narrower second barrier (TS2) is much more important, even though it is higher than TS1.[1,5,8,18] One also cannot exclude contributions from the "direct" pathway, where Mu tunneling through the higher and *much* wider barrier at TS NNOH‡ could play a role.[1,4,6,8,18] It is our suspicion though that the width of this barrier argues against significant tunneling, even in the unlikely event that the ZPE shifts should reverse the relative heights of this barrier and that of TS2, but detailed model calculations are required to establish this.

Bozzelli et al.[6] have calculated the temperature dependence for both the direct and indirect pathways for H + N_2O, based on the quantum version of Kassel theory (QRRK theory), finding essentially the same "*A*" factors but quite different activation energies, 76.6 and 56.7 kJ/mol, respectively. If their arguments were valid for the Mu analogue, the indirect path at temperatures less than 700 K would be favored by 2 orders of magnitude, consistent with earlier statements. Given the facile nature of Mu to exhibit quantum tunneling, however, we can expect this difference to be much more enhanced for the Mu + N_2O reaction, not just because of the difference in barrier heights, each of which could be shifted to higher values resulting from ZPE shifts at the TS, but particularly because of the *widths* of the barriers. The tunneling effect in the indirect pathway is most obvious at low pressures, where the decomposition channel dominates; the upward curvature at low temperature in Figure 9 is characteristic of tunneling. At high pressures, the contribution from tunneling is much less and hence the degree of curvature is less. Although the large KIE may be partly due to ZPE effects at the intermediate and the second barrier, the temperature dependence of both the rate coefficients and the KIE is consistent with a tunneling effect. While the above arguments must await confirmation from theory, we feel confident that the pronounced curvature seen in the Arrhenius plots for the Mu reaction at both low (where the H atom also exhibits some tunneling) and high pressures is dominated by the indirect pathway and *not* due to a change in mechanism (from indirect to direct pathway).

One may also expect the addition channel to be subject to tunneling. However, the overall effect on k_{add} is likely small (see Figure 10), not only because of the greater width of the first barrier (TS1) but also because tunneling goes in both directions, i.e., both k_a and k_{-a} would increase. In fact, the expected temperature dependence of the dissociation step (k_{-a}) in the addition reaction is so large that it causes the Arrhenius plot to curve downward at higher temperatures, in marked contrast to the effect of tunneling on k_{dec} discussed above (Figure 9). This effect can be seen clearly in Figure 10 which plots the Arrhenius dependence of k_{add} at 1 atm, comparing the Mu results with the *calculated* H(D) values.[5] Normally, Arrhenius plots are straight or curve upward, as seen in Figure 9 for the decomposition channel. Note also that at higher temperatures, the isotope effect is reversed for the addition channel, favoring the heavier isotope, first H and then, at even higher temperatures,

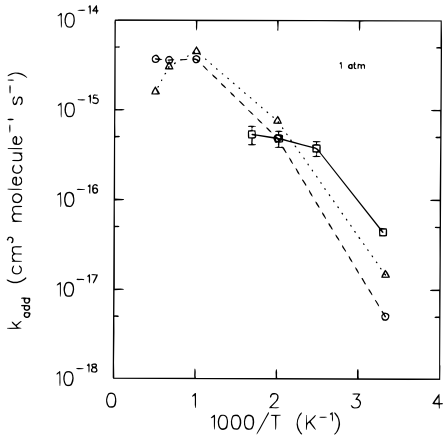

Figure 10. Arrhenius plot of the addition rate coefficient for the Mu + N_2O reaction at 1 atm total (N_2O) pressure (squares, solid line) compared with the theoretical calculations for the H (triangles, dotted line) and D (circles, dashed line) reactions at the same pressure.[5]

TABLE 4: Activation Energy (E_a in kJ/mol) for Mu(H,D) + N_2O

temp range (K)	Mu	H[a]	D[a]
300−500	3.9[b]	19	30
500−1000	23[c]	70	76

[a] Calculated from the two-term fits given in ref 1. [b] Temperature range is 300−400 K. [c] Temperature range is 400−600 K.

deuterium. This is a particularly interesting dynamical mass effect, the temperature dependence of which is reported here in the Mu case for the first time. (In our recent reported study of Mu + NO,[22] an inverse KIE of this nature favoring H over Mu was observed, but only at room temperature.) This downward curvature of the addition rate coefficient k_{add} (Figure 10) cancels the tunneling effect in k_{dec}, rendering the Arrhenius plot for the total rate coefficient almost linear at higher pressures (Figures 8 and 9).

This interpretation is consistent with an expected enhancement in $k_{-a}(T)$, from RRKM or even simpler theories of unimolecular dissociation,[26,22] but awaits confirmation from specific theoretical calculations of effects of this nature, as does our recent Mu + NO study.[22]

In summary, the overall dramatic KIE reported here is mainly a result of the pronounced enhancement in tunneling in the Mu + N_2O reaction compared to H(D) + N_2O. While tunneling through both barriers of the indirect pathway could be contributing, the narrower barrier at the second transition state (TS2) argues that tunneling is primarily via k_d in the definition of k_1 in eq 1 (contributions from k'_d, via the direct pathway are thought unlikely). At high temperatures, the isotope effect is much smaller since tunneling is less important. At high pressures, the isotope effect in the overall rate coefficient due to tunneling is also reduced because of the increased stabilization probability of the MuNNO* intermediate. By fitting the three higher-temperature points (400−600 K) and the two lower-temperature points (300−400 K) of the total rate coefficients for Mu + N_2O at 200 Torr, respectively, to the simplest form of the Arrhenius equation, activation energies (E_a) for the two temperature ranges were estimated. These are listed and compared in Table 4 with those determined from the two-term fit to the low-pressure H(D) + N_2O experimental data given in ref 1. The activation energies at lower temperatures are considerably reduced compared with those at higher temperatures in *all* three reactions (Figure 7, Table 4), with the relative magnitudes of the temperature dependence of E_a increasing with decreasing mass, and those for Mu + N_2O are *much* smaller

than those for H(D) + N_2O. These trends are consistent with the fact that the tunneling effect is more important at lower temperatures for lighter isotopes, a trend discussed above and noted in ref 5 as well. The only reaction reported to date with an activation energy difference greater than that reported here is our study of Mu + F_2, where at ∼100 K, E_a(Mu) → 0, the first indication of Wigner "threshold tunneling" in gases.[15] The small difference seen between E_a(H) and E_a(D) at high temperature (Table 4), where in fact E_a(D) is slightly larger, is also an indication that ZPE shifts at the TS2 are not appreciable, as expected for an early barrier on such an exothermic surface. The above comparisons are based on specific theoretical calculations of the H(D) + N_2O reactions, and the aforementioned "discrepancies" between this theory[5] and the Mu experimental data are believed to result from a much enhanced contribution from tunneling for Mu + N_2O over the temperature range of the measurements. Indications are that the theoretical calculations may in fact have *underestimated* the tunneling effect in the case of H(D) + N_2O, but there are no specific calculations for Mu + N_2O at present. Another contribution that needs to be considered is that the direct pathway may play a greater role for Mu systems than suggested above. Answers to these questions as well as a definitive explanation of the KIEs seen in comparison of Mu(H,D) + N_2O will only be forthcoming after theoretical calculations of the Mu + N_2O kinetics are carried out.

5. Conclusions

Rate coefficients for the Mu + N_2O reaction, separately determined for both addition and decomposition channels, have been measured over a range of temperatures (∼300−600 K) and pressures (∼1−60 atm) in TF μSR experiments. This is the first experimental study of the important H isotope + N_2O reaction system over such a wide range of pressure. Comparing with the H(D) reaction system, pronounced kinetic isotope effects are evident and their pressure and temperature dependences are, qualitatively, consistent with trends established in recent theoretical predictions for H(D) + N_2O.[5,6] Although the addition reaction forming MuNNO is important at high pressures, as predicted by theory, the decomposition channel forming MuO dominates at pressures below a few atmospheres at all temperatures, contrary to these same calculations for H(D)[5,6] which predict that the addition channel dominates at low temperatures. At lower temperatures, pronounced quantum tunneling is evident for the Mu reaction at lower pressures (Figure 7), which is much more dramatic than that seen in the corresponding H(D) + N_2O studies, indicating that the tunneling effect in the decomposition channel is considerably more important than the stabilization of the MuNNO* adduct. Nevertheless, the high-pressure Mu data provides the first experimental confirmation of the theoretical prediction that the formation of H(D)N_2O can be important (at lower temperatures) in H(D) + N_2O,[5,6] where one would naturally expect the addition channel to be more dominant due to reduced tunneling compared to the Mu + N_2O reaction. The present data also show (Figure 6) that the addition channel is, as shown by earlier calculations for H(D),[1] in the low-pressure (termolecular) regime over the pressure range of the Mu experiment.

Though reasonable extensions of the theoretical calculations for H(D) + N_2O can be made for the present Mu data, a confident assessment of the dramatic KIEs established in this work must await specific calculation of the Mu + N_2O reaction dynamics. In particular, an accurate knowledge of the zero-point-corrected barriers for the Mu system, properly variationally optimized, is required.

Acknowledgment. The continuing financial support of NSERC is gratefully acknowledged. The technical support of the μSR Facility at TRIUMF and the assistance of Dr. Syd Kreitzmann and Mr. Curtis Ballard was also much appreciated.

References and Notes

(1) (a) Marshall, P.; Ko, T.; Fontijn, A. *J. Phys. Chem.* **1989**, *93*, 1922. (b) Marshall, P.; Fontijn, A.; Melius, C. F. *J. Chem. Phys.* **1987**, *86*, 5540.

(2) (a) Ohoyama, H.; Takayanagi, M.; Nishiya, T.; Hanazaki, I. *Chem. Phys. Lett.* **1989**, *162*, 1. (b) Dean, A. M.; Johnson, R. L.; Steiner, D. C. *Combust. Flame* **1980**, *37*, 41. (c) Hidaka, Y.; Takuma, H.; Suga, M. *Bull. Chem. Soc. Jpn.* **1985**, *58*, 2911. (d) Glass, G. P.; Quy, R. B. *J. Phys. Chem.* **1979**, *83*, 30. (e) Dixon-Lewis, G.; Williams, D. J. *Gas-Phase Combustion*, Elsevier: Amsterdam, 1977; Chapter 1. (f) Balakhnine, V. P.; Vandooren, J.; Van Tiggelen, P. J. *Combust. Flame* **1977**, *28*, 165.

(3) Durant, J. L., Jr. *J. Phys. Chem.* **1994**, *98*, 518.

(4) Bradley, K. S.; Schatz, G. C. *J. Phys. Chem.* **1996**, *100*, 12154.

(5) Diau, E. W. G.; Lin, M. C. *J. Phys. Chem.* **1995**, *99*, 6589.

(6) Bozzelli, J. W.; Chang, A. Y.; Dean, A. M. *25th Symposium (International) on Combustion*; The Combustion Institute: Pittsburgh, PA, 1994; pp 965−974.

(7) Husain, D. *Ber. Bunsen-Ges. Phys. Chem.* **1977**, *81*, 168.

(8) Melius, C. F.; Binkley, J. S. *20th Symposium (International) on Combustion*; The Combustion Institute: Pittsburgh, PA, 1984; pp 575−583.

(9) Sausa, R. C.; Anderson, W. R.; Dayton, D. C.; Faust, C. M.; Howard, S. L. *Combust. Flame* **1993**, *94*, 407.

(10) Miller, J. A.; Melius, C. F. *24th Symposium (International) on Combustion*; The Combustion Institute: Pittsburgh, PA, 1992; pp 719−726.

(11) (a) Miller, J. A.; Branch, M. D.; Green, R. M.; Kee, R. J. *Combust. Sci. Technol.* **1983**, *34*, 149. (b) Harrison, J. A.; Whyte, A. R.; Phillips, L. F. *Chem. Phys. Lett.* **1986**, *129*, 346. (c) Mertens, J. D.; Chang, A. Y.; Hanson, R. K.; Bowman, C. T. *Int. J. Chem. Kinet.* **1991**, *23*, 173.

(12) (a) Hollingsworth, W. E.; Subbiah, J.; Flynn, G. W.; Weston, R. E., Jr. *J. Chem. Phys.* **1985**, *82*, 2295. (b) Shin, S. K.; Chen, Y.; Nickolaisen, S.; Sharpe, S. W.; Beaudet, R. A.; Wittig, C. *Adv. Photochem.* **1991**, *16*, 249. (c) Hoffman, G.; Oh, D.; Chen, Y.; Engel, Y. M.; Wittig, C. *Isr. J. Chem.* **1990**, *30*, 115. (e) Bohmer, E.; Shin, S. K.; Chen, Y.; Wittig, C. *J. Chem. Phys.* **1992**, *97*, 2536.

(13) (a) Senba, M. *Hyp. Int.* **1990**, *65*, 779. (b) Senba, M. *J. Phys. B* **1990**, *23*, 1545. (c) Fleming, D. G.; Senba, M. *Proceedings of NATO Advanced Research Workshop on Atomic Physics with Positrons*; Plenum: New York, 1987; p 343.

(14) (a) Lightfoot, P. D.; Pilling, M. J. *J. Phys. Chem.* **1987**, *91*, 3373. (b) Malins, R. J.; Setser, D. W. *J. Chem. Phys.* **1980**, *73*, 5666.

(15) Gonzalez, A. C.; Reid, I. D.; Garner, D. M.; Senba, M.; Fleming, D. G.; Arseneau, D. J.; Kempton, J. R. *J. Chem. Phys.* **1989**, *91*, 6164.

(16) Venkateswaran, K.; Barnabas, M.; Wu, Z.; Walker, D. C. *Radiat. Phys. Chem* **1988**, *32*, 65.

(17) For the sake of simplicity, the H atom will be used as the labeling isotope in the following discussion. The arguments can be equally applied to other H isotopes and in particular Mu, of interest here, with some adjustment of the numbers, notably the heats of reaction. On the basis of ZPE arguments,[23,26,38] Mu reactivity can be expected to be ∼20 kJ mol^{-1} *less* exothermic than the corresponding H atom reactions.

(18) Walch, S. P. *J. Chem. Phys.* **1993**, *98*, 1170.

(19) Troe, J. *Ber. Bunsen-Ges. Phys. Chem.* **1983**, *87*, 161.

(20) Pan, J. J. Ph.D. Thesis, University of British Columbia, Vancouver, BC, Canada, 1996.

(21) Dilger, H.; Schwager, M.; Tregenna-Piggott, P. L. W.; Roduner, E.; Reid, I. D.; Arseneau, D. J.; Pan, J. J.; Senba, M.; Shelley, M.; Fleming, D. G. *J. Phys. Chem.* **1996**, *100*, 6561.

(22) Pan, J. J.; Senba, M.; Arseneau, D. J.; Gonzalez, A. C.; Kempton, J. R.; Fleming, D. G. *J. Phys. Chem.* **1995**, *99*, 17160.

(23) Baer, S.; Fleming, D. G.; Senba, M.; Gonzalez, A. *Isotope Effects in Gas-Phase Chemistry*; American Chemical Society: Washington, D.C., 1992; Chapter 11.

(24) Fleming, D. G.; Senba, M. *Perspectives of Meson Science*; North-Holland: Amsterdam, 1992; pp 219−264.

(25) Fleming, D. G.; Senba, M.; Pan, J. J.; Arseneau, D. J. *Proceedings of the XIX ICPEAC*; AIP: Whistler, BC, 1995; p 413.

(26) Garner, D. M.; Fleming, D. G.; Arseneau, D. J.; Senba, M.; Reid, I. D.; Mikula, R. J. *J. Chem. Phys.* **1990**, *93*, 1732.

(27) Duchovic, R. J.; Wagner, A. F.; Turner, R. E.; Garner, D. M.; Fleming, D. G. *J. Chem. Phys.* **1991**, *94*, 2794.

(28) Fleming, D. G.; Pan, J. J.; Senba, M.; Arseneau, D. J.; Kiefl, R.; Shelley, M.; Cox, S. F. J.; Percival, P.; Brodovitch, J. *J. Chem. Phys.* **1996**, *105*, 7517.

(29) (a) Turner, R.; Snider, R. *Phys. Rev. A* **1996**, *54*, 4815. (b) Turner, R. E.; Snider, R. F. *Phys. Rev. A* **1994**, *50*, 4743.

(30) (a) Atherton, N. M. *Electron Spin Resonance*; Halstead: New York, 1973. (b) Weltner, W. *Magnetic Atoms and Molecules*; Nostrand Reinhold: New York, 1982; p 78.

(31) Pan, J. J.; Arseneau, D. J.; Senba, M.; Shelley, M.; Fleming, D. G. *Hyp. Int.* **1997**, *106*, 181.

(32) Arseneau, D. J.; Pan, J. J.; Senba, M.; Shelly, M.; Fleming, D. G. *Hyp. Int.* **1997**, *106*, 151.

(33) Pan, J. J.; Fleming, D. G.; Senba, M.; Arseneau, D. J.; Snooks, R.; Baer, S.; Shelley, M.; Percival, P. W.; Brodovitch, J. C.; Addison-Jones, B.; Wlodek, S.; Cox, S. F. J. *Hyp. Int.* **1994**, *87*, 865.

(34) Cox, S. F. J.; McRae, R. M.; Williams, R. M.; Fleming, D. G. *Hyp. Int.* **1994**, *87*, 871.

(35) Pan, J. J.; Senba, M.; Arseneau, D. J.; Kempton, J. R.; Fleming, D. G.; Baer, S.; Gonzalez, A. C.; Snooks, R. *Phys. Rev. A* **1993**, *48*, 1218.

(36) Senba, M.; Pan, J. J.; Arseneau, D. J.; Baer, S.; Hahn, M.; Snooks, R.; Fleming, D. G. *Hyp. Int.* **1994**, *87*, 965.

(37) (a) Arseneau, D. J.; Hitti, B.; Kreitzman, S. R.; Whidden, E. *Hyp. Int.* **1997**, *106*, 277. (b) Beveridge, J. L.; Doornbos, J.; Garner, D. M. *Hyp. Int.* **1986**, *32*, 907. (c) Keitel, R.; Worden, J. T. *Hyp. Int.* **1986**, *32*, 901.

(38) (a) Snooks, R.; Arseneau, D. J.; Fleming, D. G.; Senba, M.; Pan, J. J.; Shelley, M.; Baer, S. *J. Chem. Phys.* **1995**, *102*, 4860. (b) Snooks, R.; Arseneau, D. J.; Baer, S.; Fleming, D. G.; Senba, M.; Pan, J. J.; Shelley, M. *Hyp. Int.* **1994**, *87*, 911.

(39) (a) Ross, S. K.; Sutherland, J. W.; Kuo, S.-C.; Klemm, R. B. *J. Phys. Chem. A* **1997**, *101*, 1104. (b) Michael, J. V.; Lim, K. P. *J. Chem. Phys.* **1992**, *97*, 3228.

(40) *CRC Handbook of Chemistry and Physics*, 59th ed.; Weast, R. C., Ed.; CRC Press: Boca Raton, FL, 1979.

(41) For pure N_2O, a linear moderator dependence means a quadratic dependence on $[N_2O]$.

(42) (a) Melius, C. F. *Chemistry and Physics of Energetic Materials*; Kluwer: Dordrecht, 1990; pp 21−49. (b) Krishnan, R.; Frisch, M. J.; Pople, J. A. *J. Chem. Phys.* **1980**, *72*, 4244.

(43) Roduner, E.; Louwrier, P. W. F.; Brinkman, G. A.; Garner, D. M.; Reid, I. D.; Arseneau, D. J.; Senba, M.; Fleming, D. G. *Ber. Bunsen-Ges. Phys. Chem.* **1990**, *94*, 1224.

(44) (a) Garner, D. M.; Fleming, D. G.; Mikula, R. J. *Chem. Phys. Lett.* **1985**, *121*, 80. (b) Reid, I. D.; Garner, D. M.; Lee, L. Y.; Senba, M.; Arseneau, D. J.; Fleming, D. G. *J. Chem. Phys.* **1987**, *86*, 5578.